JOURNAL OF MATERIALS SCIENCE 29 (1994) 4244–4251

Study of lanthanum-based colloidal sols formation

P. CHANAUD, A. JULBE*, P. VAIJA, M. PERSIN, L. COT
Laboratoire de Physicochimie des Matériaux (URA 1312 CNRS), Ecole Nationale Supérieure de Chimie, 8 Rue de l'Ecole Normale, 34053 Montpellier Cedex 1, France

Lanthanum-based colloidal sols have been studied in order to synthesize lanthanum oxychloride inorganic coatings or thin layers for catalytic applications. The singularity of this process leading to microporous coatings is based on the polymerization of lanthanum acetate species in aqueous solution. Sols are prepared from lanthanum chloride modified by acetate ions. The sol formation mechanism can be explained by La^{3+} hydrolysis, giving basic species ($La(OH)_x$ with $x = 1$ or 2) which condense and lead to polycondensed hydroxo ions. In the pH range of sol formation, OH^- and CH_3COO^- are ligands competitive towards La^{3+}; when acetate ions are present, the condensation rate is limited by lanthanum acetate complexation. Several distributions of lanthanum hydroxide and acetate species are given and related to experimental results (pH, Fourier transform infrared (FTIR) spectroscopy, turbidity and stability of sols, SEM and TEM analysis of coatings). FTIR spectroscopy has been revealed as useful to evidence a polymerization of acetate species in sols leading to translucent gels. These gels allow the preparation of almost fully dense LaOCl coatings after thermal treatment above 450 °C. These results confirm the possible polymerization of lanthanum acetate complexes during the drying step and emphasize the great effect of acetate species on the final material texture.

1. Introduction

The interest of lanthanide compounds for catalytic applications and especially for methane activation is widely recognized [1]. Nevertheless little attention has been focused on the preparation and properties of lanthanum oxychloride powders [2] or thin films. This oxychloride compound is somewhat interesting compared to the pure oxide La_2O_3 which is very sensitive to both carbonation and hydration [3], and consequently unstable in an air atmosphere. LaOCl is much more stable and its catalytic activity has been already demonstrated for oxidative coupling of methane reactions [4–6]. The recent interest in catalytic membrane reactors [7, 8] has created a need for catalytically active membranes. In this framework the preparation of LaOCl membranes is of particular interest. In order to reach this objective we have chosen to investigate the sol–gel process from an $LaCl_3$ precursor. The purpose of this work is to focus on the sol–gel process parameters leading to the preparation of homogeneous LaOCl thin films with specific texture. A relation between theoretical data concerning the possible existing species in aqueous solution and the experimental results will be sought in order to better control the film morphology.

2. Experimental procedure

2.1. Sol preparation

A defined volume of ammonium acetate solution ($C_a = 2.70$ M) was added to a lanthanum chloride (Fluka) solution. The sol formation was carried out by rapidly adding a desired amount of dilute ammonia ($C_b = 1.00$ M) to the previous solution under stirring. Three parameters have been identified which control the sol formation: the molar ratio $CH_3COO^-/La^{3+} = A$, the molar ratio $NH_3/La^{3+} = B$, and the total lanthanum concentration C.

In order to prepare the sols an alternative process can be used which involves the use of lanthanum chloride with acetic acid. In this case ammonia has two functions which are the neutralization of acetic acid and the sol formation. However, the neutralization point of acetic acid by ammonia is difficult to reach precisely and for this reason the first described process is much more accurate. All the sols can be stabilized by polyvinylic alcohol (PVA) which is also used as a binder for thin film deposition. PVA acts as a dispersing agent for the highly concentrated sols by means of steric interactions, whereas an electrostatic stabilization mechanism is not sufficient. The stirring time has to be precisely controlled for a good homogenization of sols. In order to study the potentialities of these sols for thin film preparation, the sols were slip-cast on to flat glass substrates, dried at 25 or 110 °C under a nitrogen atmosphere and heat-treated at 450 °C.

2.2. Sol and thin film characterizations

In most cases sol characterization presented some difficulties because they were turbid, concentrated and

* To whom all correspondence should be addressed.

0022–2461

viscous. Furthermore, thixotropy was very important in the most concentrated ones. Turbidity measurements were made with a Hach turbidimeter (Ratio/XR) calibrated with four different Gelex gels in the 0–2000 NTU scale. Fourier transform infrared (FTIR) spectra were obtained with a Nicolet 5ZDX spectrophotometer. The textures of the heat-treated deposits were examined by scanning electron microscopy (SEM) (Cambridge Stereoscan 250) and transmission electron microscopy (TEM) (Jeol 100 CX).

3. Results and discussion

3.1. Behaviour of lanthanum salts in aqueous media ($A = 0$)

In order to describe the reaction mechanisms involved in sol formation, we have to consider the properties of lanthanum ions in aqueous solution. La^{3+} presents a noble gas valency shell configuration and its ionic radius (0.106 nm) is quite large compared to those of other trivalent ions [9]. This implies that its ionic potential (charge to radius ratio) is quite low. The ionic character of the metal–ligand bond predominates, involving a low energy level and a coordination number greater than six (the usual coordination number for d-elements). Thus La^{3+} is a "hard" Pearson acid and can easily form complexes with oxygen donor ligands. Water, hydroxide, organic acids and chelating agents are particularly strong ligands toward La^{3+}. Ligands with only nitrogen donor sites (NH_3 for instance) do not form any complex with La^{3+} in aqueous solution. From the literature, the hydration number of La^{3+} increases from 9 in aqueous concentrated solutions [10] to 12 in infinite dilute solutions [11]. The hydrolysis (or aquoacidity) of lanthanum ions occurs simply by the successive departure of protons from the hydrated ion. The first step can be written as

$$[La(OH_2)_9]^{3+} \rightleftharpoons [La(OH)(OH_2)_8]^{2+} + H^+$$

When the pH increases (B i.e. increases) additional protons are lost from the coordinated water, resulting in the formation of successive basic ions or aquohydroxoions. The corresponding reactions can be written in a simplified way by omitting the coordinated water:

$$La^{3+} + H_2O \rightleftharpoons [La(OH)]^{2+} + H^+ \qquad (\log K_1 = -8.5)$$

$$[La(OH)]^{2+} + H_2O \rightleftharpoons [La(OH)_2]^{+} + H^+ \qquad (\log K_2 = -8.7)$$

$$[La(OH)_2]^{+} + H_2O \rightleftharpoons La(OH)_3 + H^+ \qquad (\log K_3 = -8.7)$$

$$La(OH)_3 + H_2O \rightleftharpoons [La(OH)_4]^{-} + H^+ \qquad (\log K_4 = -11.0)$$

The equilibrium constants K_i [12] are in fact acidity-like constants. The three first equilibria are representative of the reactions involved in hydroxide formation in dilute aqueous solution. The equilibrium constants allow one to calculate the distribution diagrams of lanthanum species (in percentages) as a function of pH (Fig. 1) by means of the following equation (independent of C):

$$\left[La(OH)_n^{(3-n)^+}\right] = 100\,\frac{10^{\,n\mathrm{pH}+\sum_{i=1}^{i=n}\log_{10}K_i}}{1+\sum_{n=1}^{n=4}10^{\,n\mathrm{pH}+\sum_{i=1}^{i=n}\log_{10}K_i}}$$

For example

$$[La^{3+}] = \frac{100}{1+10^{\mathrm{pH}-8.5}+10^{2\mathrm{pH}-17.2}+10^{3\mathrm{pH}-25.9}+10^{4\mathrm{pH}-36.9}}$$

$$[La(OH)^{2+}] = \frac{100\times10^{\mathrm{pH}-8.5}}{1+10^{\mathrm{pH}-8.5}+10^{2\mathrm{pH}-17.2}+10^{3\mathrm{pH}-25.9}+10^{4\mathrm{pH}-36.9}}$$

No hydrolysis occurs in an acidic medium and 100% of lanthanum is in the $(La^{3+})_{aq}$ form. Hydroxide precipitation is complete at pH around 10. Hydroxide is slightly soluble in a strongly basic medium because of the existence of $[La(OH)_4]^-$. Hydrolysis begins when

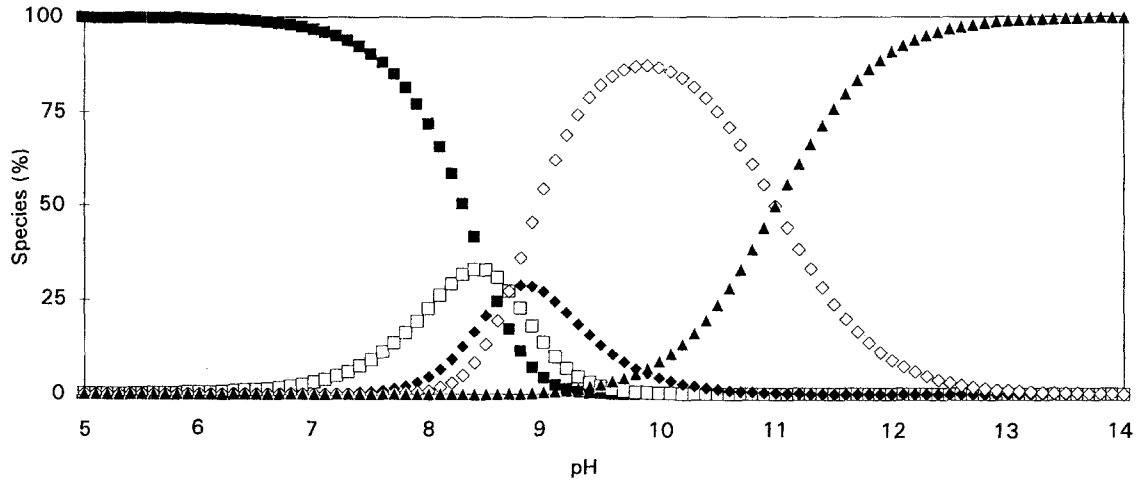

Figure 1 Distribution of lanthanum species as a function of pH ($A = 0$): (■) La^{3+}, (□) $[La(OH)]^{2+}$, (◆) $[La(OH)_2]^{+}$, (◇) $La(OH)_3$, (▲) $[La(OH)_4]^{-}$.

the pH is greater than 6. Two basic species, $[La(OH)]^{2+}$ and $[La(OH)_2]^{+}$, predominate in a short pH range around 8.5. This kind of graph (Fig. 1), which is mainly valid in dilute solutions, allows a first approach to lanthanum behaviour in an aqueous solution.

In more concentrated solutions a condensation phenomenon takes place, beginning with the condensation of two basic species through hydroxy bridge formation. The first step of this process may be condensation of the first-generated basic species with the initial hydrated ion according to the reaction

$$[La(OH_2)_9]^{3+} + [La(OH)(OH_2)_8]^{2+} \rightleftharpoons \left[(H_2O)_8La\overset{H}{\underset{|}{O}}La(OH_2)_8\right]^{5+} + H_2O$$

This reaction can also be written in a simpler way

$$La^{3+} + [La(OH)]^{2} \rightleftharpoons [La_2(OH)]^{5+}$$

This condensation goes on with polynuclear species formation whose general formulae can be written as $[La_q(OH)_p(OH_2)_x]^{(3q-p)+}$.

According to our experiments, sol formation occurs through this condensation process (called olation) in the pH range (7–8.5) corresponding to the formation of the two basic species as predicted in Fig. 1. Two polynuclear species have been proposed by Biedermann and Ciavatta [13] from modelling data; their (p, q) values are (1, 2) and (9 or 10, 5 or 6). The values (1, 2) correspond to the first condensation step previously described and leading to $[La_2(OH)]^{5+}$. With increasing pH the polynuclear species lose protons (and water) according to the reaction.

$$[La_q(OH)_p(OH_2)_x]^{(3q-p)+} \rightleftharpoons La_q(OH)_{3q}(OH_2)_y + (3q - p)\,H^+$$

and their formulae tend to the hydroxide stoichiometry $La_q(OH)_{3q}(OH_2)_y$. Some authors [14–16] have pointed out that some basic salts could be formed and precipitated before the hydroxide. In our case, in the presence of chloride species, two basic species have to be considered: $La(OH)_aCl_b$ with (a, b) equal to (2, 1) and (2.5, 0.5).

As a first conclusion we can say that when increasing the pH of a starting solution of concentrated lanthanum chloride, hydrolysis begins with the formation of some basic ions which condense in order to form condensed species (a sol). These species can hydrolyse by losing protons and precipitate in hydroxide or basic salt form.

We have established that the rate of ammonia addition (dropwise or in one step) clearly influences sol

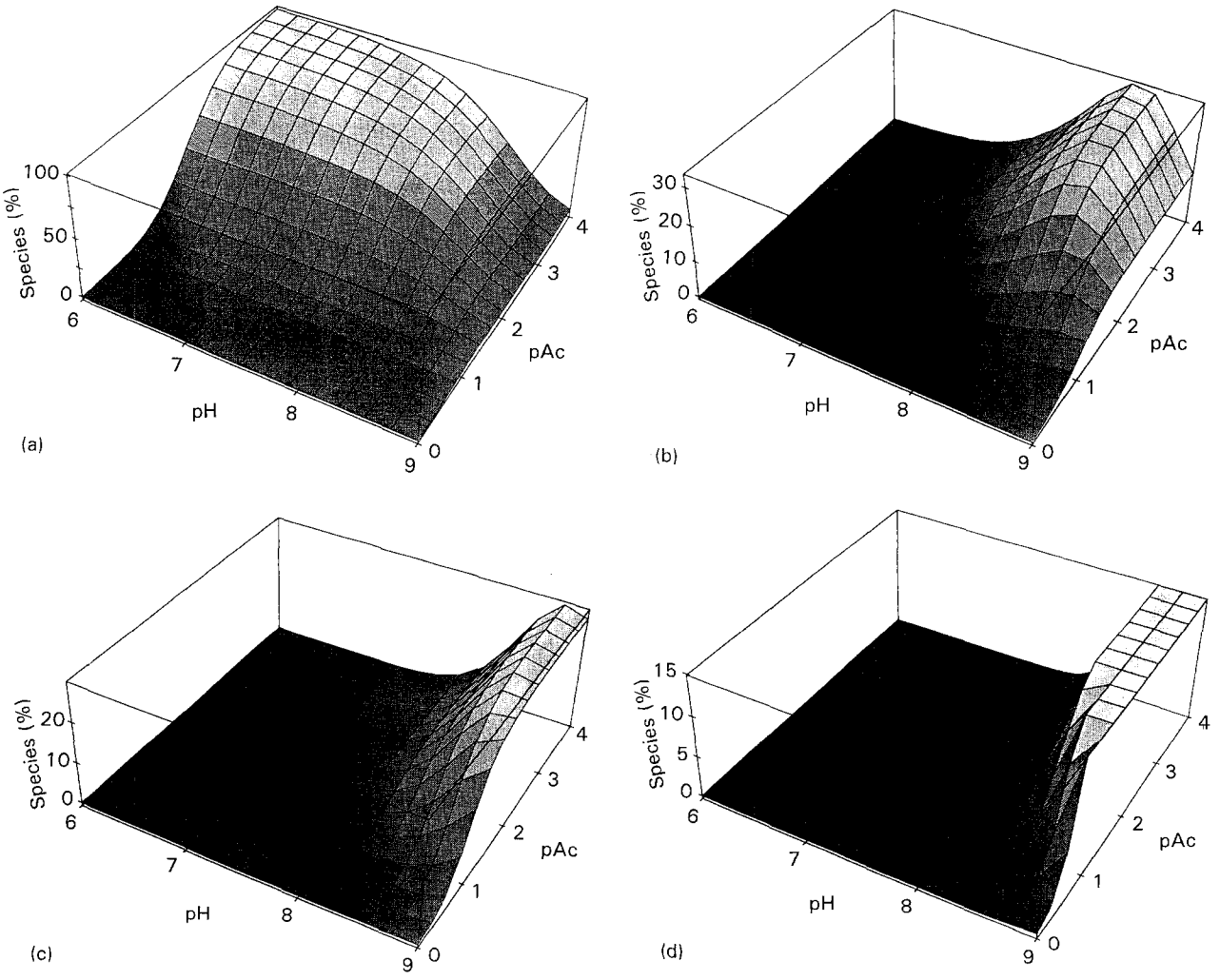

Figure 2 Distribution of lanthanum species as a function of pH and pAc: (a) La^{3+}, (b) $[La(OH)]^{2+}$, (c) $[La(OH)_2]^{+}$, (d) $La(OH)_3$.

homogeneity. Colloidal particles are formed through the nucleation of embryos (at first statistical and unstable associations of polynuclear species) which grow up to a stable particle size. By adding the desired amount of ammonia in one step, hyrolysis is forced to occur by reaching a supersaturation level (i.e. a finite number of condensed basic ions are formed in one step which can then grow homogeneously up to a defined size). If ammonia is added dropwise, some nuclei are formed by the first drops and the next drops allow them to grow while new nuclei can also be formed. Inhomogeneous sols result from this last procedure.

By controlling the parameters B and C and the rate of ammonia addition, hydrolysis and condensation reactions can be monitored. Sols are obtained for $B < 3$ and more stable sols for $B < 2$. For the same amount of ammonia added to lanthanum chloride solutions with various concentrations C, stable sols can be obtained for high C values ($C \geqslant 1$ M). Indeed in this case the NH_3/La^{3+} ratio is low enough to favour the basic species responsible for sol formation.

3.2. Effect of acetate ion ($A \neq 0$)

We have noticed that acetate ions have a specific action on sol formation, resulting in smaller particles. Four kinds of lanthanum acetate complex can be found in the literature [17] and the equilibrium constants for the formation of $[La(Ac)_n]^{(3-n)+}$ are respectively $\log\beta_n = 2.0, 3.3, 3.0$ and 2.9 for $n = 1, 2, 3$ and 4. By considering the four kinds of hydroxide complex and these four kinds of acetate complex we can plot in three dimensions the species distribution diagrams (in percentages) as a function of pH and pAc by using the functions

$$[La^{3+}] = \frac{100}{1 + \sum_{n=1}^{n=4} 10^{n.pH + \sum_{i=1}^{i=n} \log_{10} K_i} + \sum_{m=1}^{m=4} 10^{\log_{10}\beta_m - m\,pAc}}$$

$$[La(OH)_n^{(3-n)+}] = [La^{3+}]10^{npH + \sum_{i=1}^{i=n} \log_{10} K_i}$$

$$[La(Ac)_m^{(3-m)+}] = [La^{3+}]10^{\log_{10}\beta_m - m\,pAc}$$

These equations are independent of C and do not consider condensed species. The results are given in Figs 2 and 3. By analogy with $pH = -\log_{10}[H^+]$, the pAc parameter is defined as $pAc = -\log_{10}[CH_3COO^-]_{free}$ where $[CH_3COO^-]_{free}$ is the free acetate ions concentration. $pAc = 4$ (i.e. $[CH_3COO^-]_{free} = 10^{-4}$ M) corresponds to a very low acetate ion concentration which is not sufficient to form complexes with lanthanum. In all the three-dimensional maps the $pAc = 4$ plane is equivalent to the

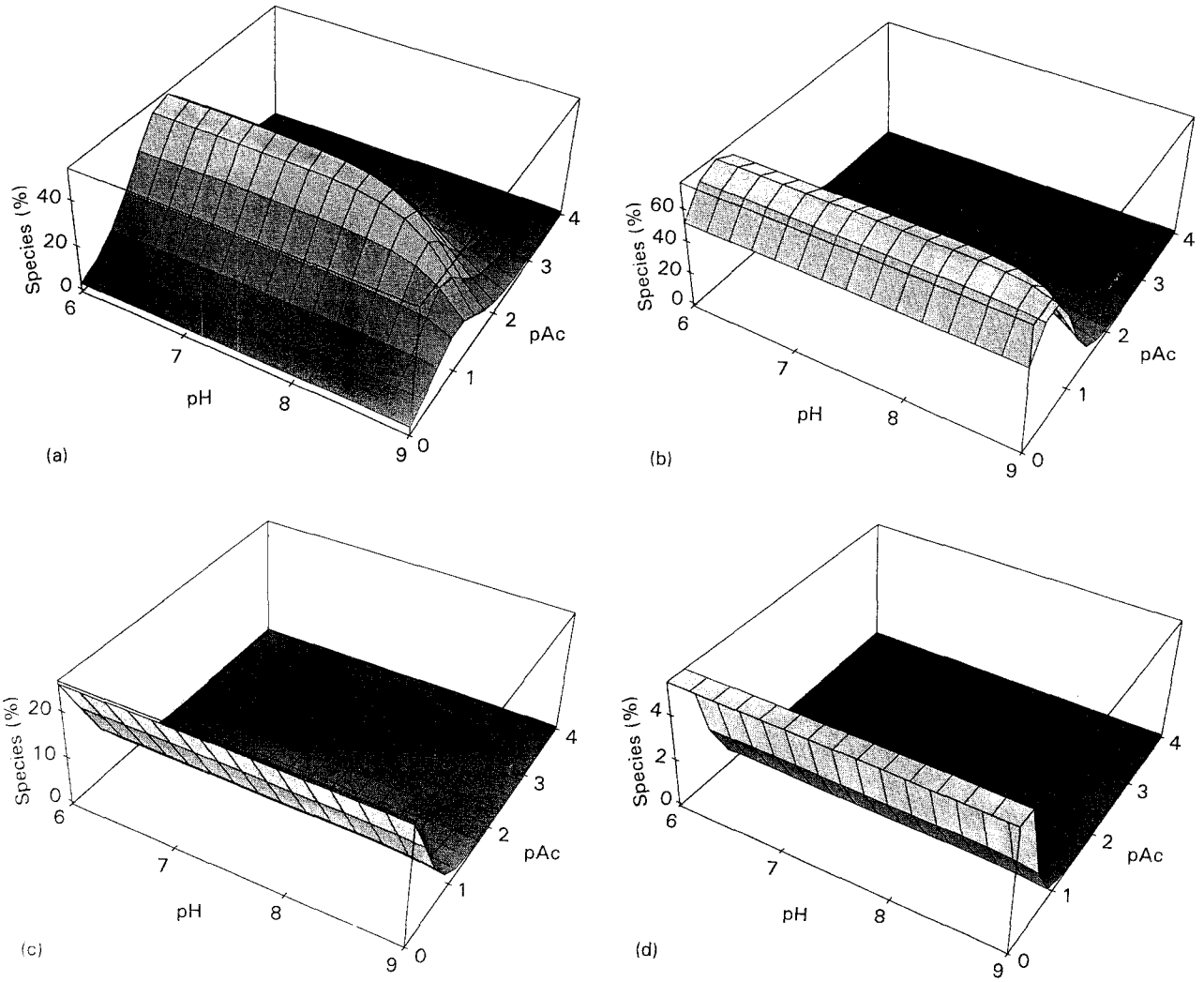

Figure 3 Distribution of lanthanum acetate species as a function of pH and pAc: (a) $[La(Ac)]^{2+}$, (b) $[La(Ac)_2]^+$, (c) $La(Ac)_3$, (d) $[La(Ac)_4]^-$.

case without complexing agent described in Fig. 1. The pH and pAc ranges represented are respectively 6–9 and 0–4, they correspond to the more useful range deduced from our experimental screening for sol preparation.

General tendencies can be deduced from Figs 2 and 3: with increasing pH, basic ions are formed which create the sol, and with decreasing pAc, acetate ions form complexes with lanthanum. In fact in the sol formation range, CH_3COO^- and OH^- are ligands competitive toward lanthanum. The La^{3+} concentration (Fig. 2a) decreases from 100 to 0% when the pH increases from 6 to 9 (basic ion formation) or when pAc decreases from 4 to 0 (acetate ion formation). The basic ion distribution maps show a maximum at pH = 8.4 for $La(OH)^{2+}$ (Fig. 2b) and at pH = 8.8 for $La(OH)_2^+$ (Fig. 2c). The maximum for $La(OH)_3$ is at pH = 9.9 (Fig. 2d) and is not shown in the chosen scale; the $La(OH)_4$ concentration is very low (< 0.04%) at pH = 9 and pAc = 4. The map for the acetate complex $La(Ac)^{2+}$ (Fig. 3a) shows a maximum (50%) at pAc = 1.8, but with increasing pH the percentage of this complexed form decreases. The same effect is observed for the $La(Ac_2)^+$complex (Fig. 3b) but shifted to low pAc values. The concentrations of $La(Ac)_3$ and $[La(Ac)_4]^-$ species are less sensitive toward pH in the studied field (Fig. 3c and d).

In order to correlate the theoretical data with our experiments, we have reported in Fig. 4 the calculated relationships between pH, pAc, and our experimental parameters A and B, while keeping C constant (C = 0.135 M). In Fig. 4a we notice that pH increases a lot from B = 0 to 0.2. This effect is decreased after B = 0.2 because of basic ion formation. The singular behaviour of the B = 0 curve is due to the buffer effect of free ammonium acetate. For any B value greater than or equal to 0.2, A has a slight effect on pH; the maximum pH is observed for A = 2. Experimentally, we observed similar results with flatter curves shifted towards lower pH values (about 0.6 unit of pH). This difference, corresponding to a greater OH^- consumption, can be explained notably by the forced hydrolysis performed in our experimental procedure. Furthermore the theory does not take into account the formation of condensed polynuclear species, the possible hydrolysis of acetate species and the effect of chloride species. In Fig. 4b it is shown that pAc decreases when A increases. The effect of B on pAc is more important for low A values, becoming negligible for high A values. An example of species distribution, namely $[La(Ac)]^{2+}$, is reported in Fig. 5. Several species coexist for given values of A and B and for this reason a maximum of 50% of lanthanum is in the $[La(Ac)]^{2+}$ form.

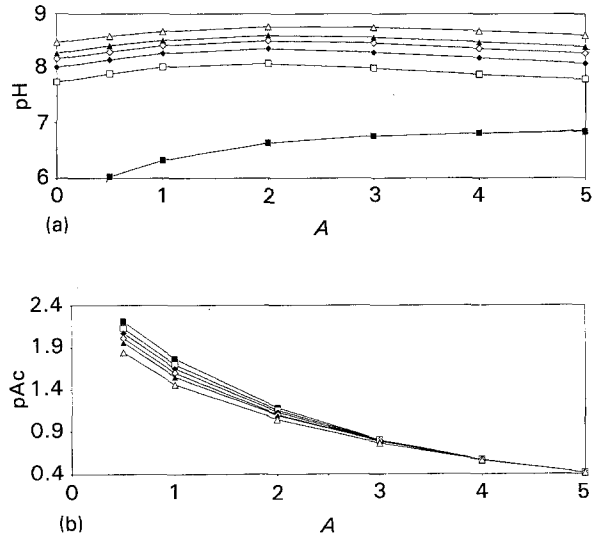

Figure 4 Theoretical evolution of (a) pH and (b) pAc as a function of A for several B values: (■) 0, (□) 0.2, (◆) 0.4, (◇) 0.6, (▲) 0.8, (△) 1.3.

3.3. Effect of total lanthanum concentration C

Let us focus now on the first step of the sol formation corresponding to low B values. When A and B are too low for complete lanthanum acetate or hydroxide formation, all lanthanum remains in solution. For A = 1 and B = 0 the species distribution as a function of C is reported in Fig. 6a. Even for high C values

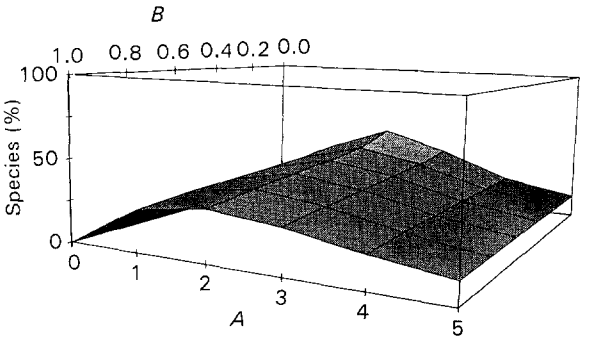

Figure 5 Distribution of $[La(Ac)]^{2+}$ as a function of A and B.

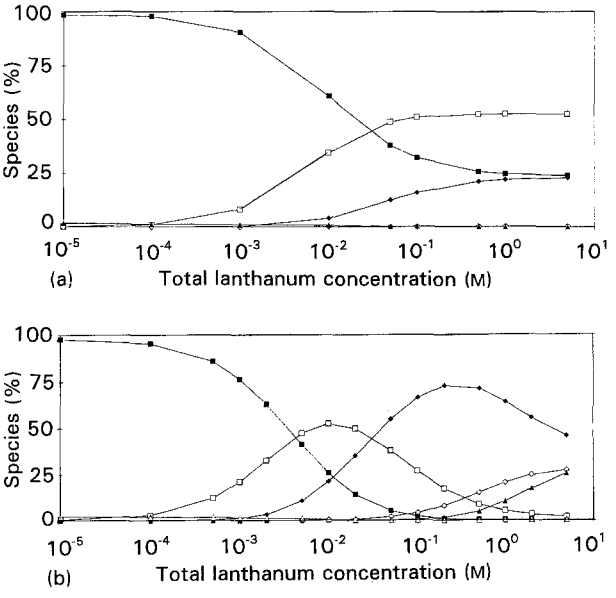

Figure 6 Distribution of lanthanum species as a function of C. (a) A = 1, B = 0: (■) La^{3+}, (□) $[La(Ac)]^{2+}$, (◆) $[La(Ac_2)]^+$, (◇) $La(Ac)_3$, (▲) $La(OH)_n$. (b) A = 3, B = 0: (■) La^{3+}, (□) $[La(Ac)]^{2+}$, (◆) $[La(Ac_2)]^+$, (◇) $La(Ac)_3$, (▲) $[La(Ac)_4]^-$, (△) $La(OH)_n$.

translucent gels are obtained because the precipitation of $LaAc_3$ or $LaOH_3$ is not possible. In the case of $A = 3$ and $B = 0$ (Fig. 6b) the $LaAc_3$ distribution increases, reaching 30% of C, and it is more difficult to avoid particle growth due to acetate precipitation. We have noticed that these conclusions can be directly applied to the drying step of the sols. Indeed an increase of C corresponds to a loss of water and different film textures can be obtained through this step.

3.4. Experimental consequences

3.4.1. Turbidity

Fig. 7 represents the evolution of turbidity τ as a function of A and B ($C = 0.135$ M). An empirical function such as $\tau(A, B) = f(A)\,B$, where $f(A)$ is a function of A, describes all our experimental values in the case of $0 < A < 5$ and $0 < B < 1.3$. Turbidity is a linear function of B. It implies that the formation and/or growth of the particles depend on the pH. For $A = 0$, once the first basic ions are formed, polycondensation reactions occur leading rapidly to a very turbid sol. A 2000 NTU value, corresponding to a milky sol, is obtained for $B = 0.55$. When A increases, $f(A)$ decreases and the turbidity level obtained is lower than 800 NTU, even for $B = 1.3$. This can be related to the fact that the polycondensation rate is limited by acetate complexation. The function $f(A)$ can be considered as resulting from the sum of different phenomena. First from $A = 0$ to 1 there is a decrease of turbidity due to a decrease of basic ion concentration. Then there is a contribution of acetate complexes which seem to hydrolyse or polymerize. Comparison of the $[LaAc]^{2+}$ distribution curve obtained with non-condensed species constant (Fig. 5) and the turbidity evolution curve (Fig. 7) reveals a very similar behaviour. A slight difference is observed which can be explained by the B dependence, this seems to confirm the hydrolysis of lanthanum acetate complexes.

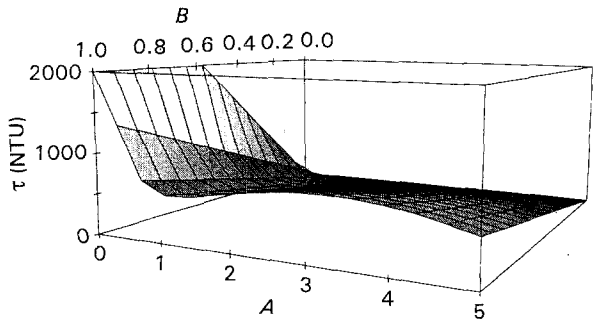

Figure 7 Evolution of turbidity τ as a function of A and B.

3.4.2. Sol stability

The stability studies revealed that sols with $A = 0$ are stable after 2 h but collapse before 7 days. The particles in these sols are the biggest of all the prepared sols; electrostatic interactions are not sufficient to repel them and coagulation systematically occurs. With $A = 0.5$ and $B > 0.2$ the sols are the most stable and never settle under gravity, the resulting gels always being thixotropic. Gelation times are quite long (several days) and decrease with B. For $A > 1$ the stability decreases because the ionic strength is too high and a phase separation is observed after 2 h.

3.4.3. FTIR analysis

The existence of lanthanum acetate complexes can be confirmed by infrared spectral analysis. The specific i.r. absorption bands of acetate species reported in the literature [18] are listed in Table I and compared with our experimental data. As shown in Fig. 8a our sols presented two strong bands at 1543 ± 2 and $1450 \pm 2\ cm^{-1}$ corresponding to ν_8-antisymmetric and ν_3-symmetric vibrations of the carbon–oxygen bond in lanthanum acetate complexes. In aqueous ammonium acetate solution, the acetate carboxy bond values are 1560 and $1419\ cm^{-1}$. These two latter bands are slightly present in our sol spectra and reveal the existence of uncomplexed acetate ions.

The acetate ion is able to coordinate in three different ways as illustrated in Fig. 9 [19]. These coordination modes can be correlated with the frequency differences $\Delta_{asym,sym}$ between the asymmetric and symmetric $-CO_2^-$ stretching vibrations. Because the lanthanum–acetate bond is mainly electrostatic there is a small difference between the three coordination modes Indeed, as reported by Karraker [18] the $\Delta_{asym,sym}$ values are respectively 85–95, 95–105 and 95–110 cm^{-1} for monodentate, bidentate and polymeric acetate ligands coordinated to lanthanide ions in crystalline lanthanide acetate. In our sols we found $\Delta_{asym,sym} \simeq 95\ cm^{-1}$, which means that the lanthanum coordination may be monodentate and/or bidentate. Polymerically coordinated aetates involve both La–O and La–O–La coordinations and induce

TABLE I Absorption bands of acetate species

		$\nu_{asym_{(coo)}}$ (cm^{-1})			$\nu_{sym_{(coo)}}$ (cm^{-1})		Source
$[La(Ac)_3 \cdot 1.5H_2O$	(crystal)	1555			1445		[18]
$[La(Ac)_3]$	(crystal	1602	1525	1470	1452	1432	[18]
Ammonium acetate	(aqueous sol)	1560				1419	Exp.
$A = 1, B = 0$	(aqueous sol)	1560	1542		1452	1419	Exp.
$A = 1, B = 0$	(dry gel)	1552	1534/1520	1470	1452	1441	Exp.
$A = 3, B = 0$	(aqueous sol)	1558	1543		1452	1423	Exp.
$A = 3, B = 0.5$	(aqueous sol)	1558	1543		1452	1423	Exp.
$A = 5, B = 0$	(aqueous sol)	1558	1545		1448	1425	Exp.

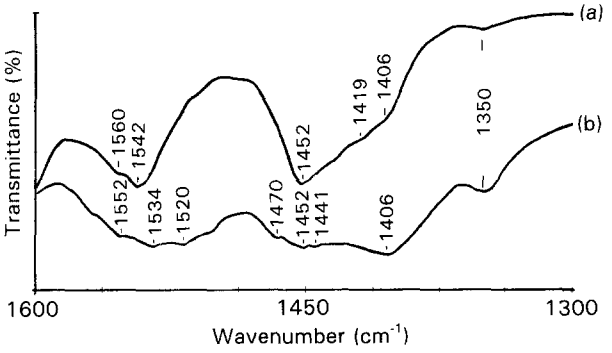

Figure 8 FTIR spectra of $A = 1$ and $B = 0$ samples (a) in aqueous solution and (b) after drying (translucent gel).

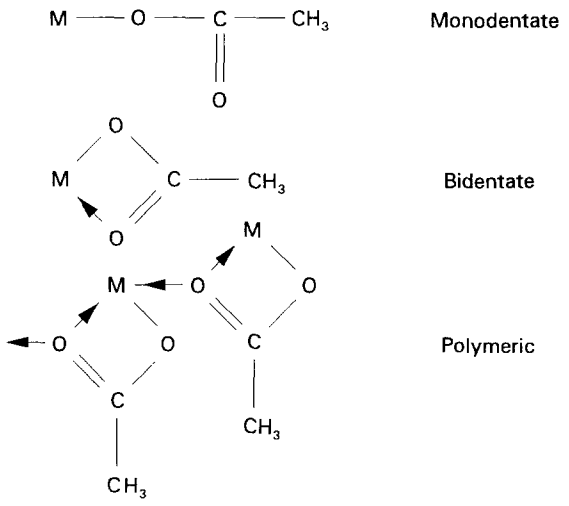

Figure 9 Possible acetate coordination on metals.

a split of the two stretching vibrations as in anhydrous $LaAc_3$ [18]. This split is not observed in our sols, even during ageing. Indeed when particles are growing in the bulk sol, no significant evolution of the bands is observed. This means that acetate remains complexed with lanthanum while the olation reaction occurs. In the case of thin film preparations a different behaviour is observed. Indeed, during the drying step and especially in cases of translucent gels (e.g. $A = 1$, $B = 0$) a split of the $-CO_2^-$ stretching vibrations is observed (Fig. 8b) corresponding to a polymerization of acetates. This typical behaviour is systematically observed in the case of translucent gels and has drastic textural consequences as shown hereafter.

3.4.4. SEM and TEM

Electron microscopy has been used in order to study the morphological aspects (particle, size and texture) of various slip-cast sols, treated at 450 °C. For $A = 0$, particles 100 nm in diameter were observed which were agglomerated (Fig. 10) due to the low stability of the corresponding sols. Nevertheless the use of PVA allowed a very good dispersion of sols, resulting in homogeneous coatings. For $A = 0.5$ and $B > 1$ homogeneous coatings were obtained with or without PVA; this composition corresponds to very stable sols.

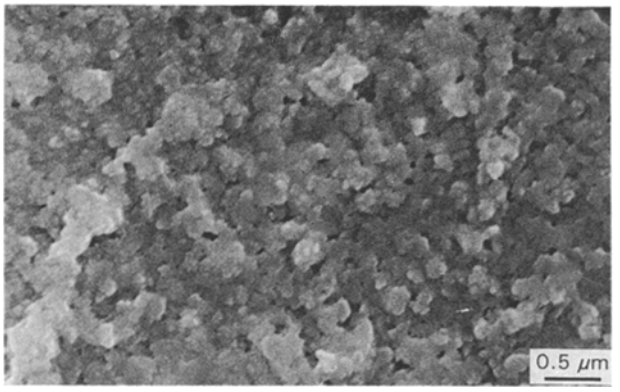

Figure 10 SEM micrograph of agglomerated LaOCl particles ($A = 0$, $B = 0.8$, $C = 0.135$ M)

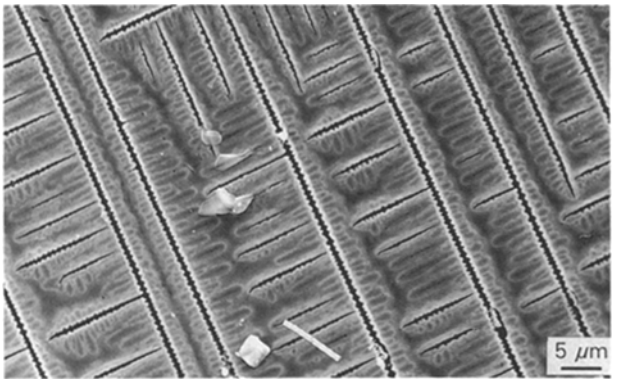

Figure 11 Oriented defects generated by the NH_4Cl dendritic crystallization and observed after thermal treatment (450 °C).

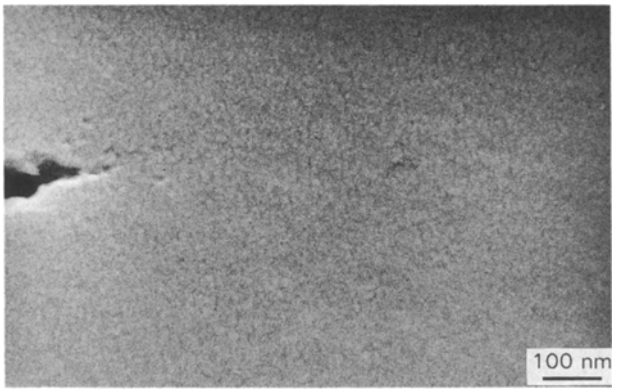

Figure 12 SEM observation of the homogeneous fine-grain texture observed outside the dendritic zones.

Finally, for $A > 2$ and with a 25 °C drying step dendritic crystals appeared, growing in homogeneous fine-grain texture. These dendrites, induced by NH_4Cl crystallization, leave holes in the resulting coatings after thermal treatment (Fig. 11). The particle size outside the dendritic zones cannot be determined even at high SEM magnification (Fig. 12). This conclusion has to be related to the previous discussion concerning the polymerization of lanthanum acetate complexes. Indeed, in the corresponding sols (which are slightly turbid) colloidal particles exist but during the drying

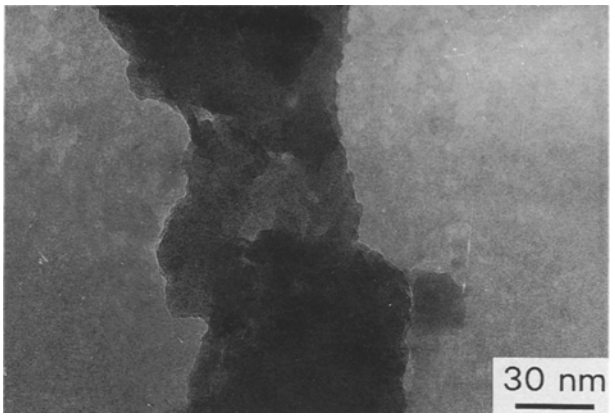

Figure 13 TEM observation of the homogeneous fine-grain texture observed outside the dendritic zones.

step a polymerization of the lanthanum acetate complexes occurs, giving microporous or dense coatings. By controlling the drying step (rapid drying at 110 °C under N_2 atmosphere) dendritic crystallization can be avoided and microporous homogeneous coatings can be obtained after the heat treatment at 450 °C. As shown in Fig. 13, the film consist of small particles about 6 nm in diameter embedded in a dense phase.

4. Conclusions

The theoretical existence of different lanthanum species in solution has been modelled and correlated with experimental parameters (*A*, *B*, *C*). We have pointed out that theoretical data are in good accordance with experimental results and can be useful to explain the sol formation. By monitoring *A*, *B* and *C* we can control the formation of the different species and consequently of different sols. By limiting the basic ion concentration low polycondensation levels are obtained, resulting in less turbid sols containing smaller colloids. Controlling the drying step allows us to synthesize homogeneous translucent gels. The infrared analysis of acetate ions in different sols allows us to distinguish between the various type of acetate ion coordination and to suggest that translucent gels are formed through acetate polymerization. We can deduce from this study that by controlling the experimental parameters, sols are obtained with different properties allowing the formation of several kinds of LaOCl coating after thermal treatment. By choosing adequate sols, homogeneous mesoporous or microporous films can be prepared, whose composition and texture are stable up to 800 °C. The application of these films to porous ceramic supports results in porous catalytic membranes, whose performance is currently being studied for the oxidative coupling of methane.

References

1. K. D. CAMPBELL, H. ZHANG and J. H. LUNSFORD, *J. Phys. Chem.* **92** (1988) 750.
2. S. TERADA, Y. HIRAI and K. KUBOTA, *Solid State Commun.* **68** (1988) 567.
3. M. P. ROSYNECK and D. T. MAGNUSON, *J. Catal.* **46** (1977) 402.
4. J. WILLIAMS, R. J. JONES, J. M. THOMAS and J. KENT, *Catal. Lett.* **3** (1989) 247.
5. A. KIENNEMAN, R. KIEFFER, A. KADDOURI, P. POIX and J. L. REHPRINGER, *Catal. Today* **6** (1990) 409.
6. A. JULBE, P. CHANAUD, A. LARBOT, C. GUIZARD, L. COT, C. MIRODATOS and H. BORGES, in "Inorganic Membranes", Key Engineering Materials Vols 61 and 62, edited by A. J. Burggraff, J. Charpin and L. Cot (Trans Tech, Zurich, 1991) p. 65.
7. H. P. HSIEH, *Catal. Rev.–Sci. Eng.* **33** (1991) 1.
8. K. KEIZER, V. T. ZASPALIS and A. J. BURGGRAFF, "Ceramics Today – Tomorrows Ceramics, part D", Materials Science Monographs, Vol. 66D (1991) p. 2511.
9. K. A. GSCHNEIDER, in "Handbook on the Physics and Chemistry of Rare Earths", edited by J. and L. Eyring (North-Holland, Amsterdam, 1979) p. 213.
10. A. HABENSCHUSS and F. H. SPEEDING, *J. Chem. Phys.* **70** (1979) 3758.
11. W. MEIER, P. BOPP, M. M. PROBST, E. SPOHR and J. I. LIN, *J. Phys. Chem.* **94** (1990) 4672..
12. J. KRAGTEN, in "Atlas of Metal Ligands. Equilibria in aqueous solution", edited by Ellis Horswood (Wiley, Chichester, 1978) p. 416.
13. G. BIEDERMANN and L. CIAVATTA, *Acta Chem. Scand.* **15** (1961) 1347.
14. N. V. AKSEL'RUD and V. B. SPIVAKOVSKI, *Russ. J. Inorg. Chem.* **5** (1960) 158.
15. N. N. MIRONOV and N. P. CHERNYAEV, *ibid.* **6** (1961) 1109.
16. L. P. MOISA and V. B. SPIVAKOVSKI, *ibid.* **15** (1970) 1513.
17. A. RINGBOM, in "Les complexes en Chimie Analytique" (Ed. Dunod, Paris, 1967) p. 297.
18. D. G. KARRAKER, *J. Inorg. Nucl. Chem.* **31** (1969) 2815.
19. A. I. GRIGOR'EV and V. N. MAKSIMJOV, *Russ. J. Inorg. Chem.* **9** (1964) 580.

Received 25 May 1993
and accepted 16 February 1994